hydrology

MDPI

Article

Groundwater Pollution Transport in Plain-Type Landfills: Numerical Simulation of Coupled Impacts of Precipitation and Pumping

Tengchao Li [1,2], Shengyan Zhang [1,2], Xiaoming Mao [1,2], Yuqin He [3], Ninghao Wang [3], Daoyuan Zheng [1,2], Henghua Gong [3] and Tianye Wang [3,*]

[1] Ecological Environment Geo-Service Center of Henan Geological Bureau, Zhengzhou 450000, China; 15136131510@163.com (T.L.); 13938487512@163.com (S.Z.); qpow97856@163.com (X.M.); 15937189839@163.com (D.Z.)
[2] Technology Research Center for Mine Environment and Ecological Restoration Engineering of Henan Province, Zhengzhou 450000, China
[3] School of Water Conservancy and Transportation, Zhengzhou University, Zhengzhou 450001, China; heyuqin@gs.zzu.edu.cn (Y.H.); wnh0501@gs.zzu.edu.cn (N.W.); gonghenghua@gs.zzu.edu.cn (H.G.)
* Correspondence: wangtianye@zzu.edu.cn

Abstract

Landfills serve as a primary disposal method for municipal solid waste in China, with over 20,000 operational sites nationwide; however, long-term operations risk leachate leakage and groundwater contamination. Amid intensifying climate change and human activities, understanding contaminant evolution mechanisms in landfills has become critically urgent. Focusing on a representative plain-based landfill in North China, this study integrated field investigations and groundwater monitoring to establish a monthly coupled groundwater flow–solute transport model (using MODFLOW and MT3DMS codes) based on site-specific hydrogeological boundaries and multi-year monitoring data, analyzing spatiotemporal plume evolution under the coupled impacts of precipitation variability (climate change) and intensive groundwater extraction (human activities), spanning the historical period (2021–2024) and future projections (2025–2040). Historical simulations demonstrated robust model performance with satisfactory calibration against observed water levels and chloride concentrations, revealing that the current contamination plume exhibits a distinct distribution beneath the site. Future projections indicate nonlinear concentration increases: in the plume core zone, concentrations rise with precipitation, whereas at the advancing front, concentrations escalate with extraction intensity. Spatially, high-risk zones (>200 mg/L) emerge earlier under wetter conditions—under the baseline scenario (S0), such zones form by 2033 and exceed site boundaries by 2037. Plume expansion scales positively with extraction intensity, reaching its maximum advancement and coverage under the high-extraction scenario. These findings demonstrate dual drivers—precipitation accelerates contaminant accumulation through enhanced leaching, while groundwater extraction promotes plume expansion via heightened hydraulic gradients. This work elucidates coupled climate–human activity impacts on landfill contamination mechanisms, proposing a transferable numerical modeling framework that provides a quantitative scientific basis for post-closure supervision, risk assessment, and regional groundwater protection strategies, thereby aligning with China's Standard for Pollution Control on the Landfill Site of Municipal Solid Waste and the Zero-Waste City initiative.

Check for updates

Academic Editor: Pantelis Sidiropoulos, Ilias Siarkos and Hailong Yin

Received: 30 October 2025
Revised: 7 January 2026
Accepted: 12 January 2026
Published: 17 January 2026

Copyright: © 2026 by the authors. Licensee MDPI, Basel, Switzerland. This article is an open access article distributed under the terms and conditions of the Creative Commons Attribution (CC BY) license.

Keywords: landfill; groundwater pollution; groundwater numerical modeling; climate change; groundwater exploitation

1. Introduction

With the continuous advancement of urbanization, China's municipal solid waste (MSW) collection volume has been growing rapidly at an annual rate of 8–10% [1,2]. For decades, landfilling has dominated urban waste disposal, supplemented by incineration and biochemical treatment [3]. In 2013, landfill, incineration, and other disposal methods accounted for 68.16%, 30.10%, and 1.74% of national MSW treatment, respectively [4,5]. Due to its relatively simple process and lower disposal costs, landfilling once served as the primary waste treatment method in China [6]. In recent years, however, incineration has gradually replaced landfilling as the dominant disposal approach, driven by the implementation of the Zero-Waste City initiative and waste classification policies [3,4]. By 2022, the proportion of landfill disposal had decreased to 12.5% [4,7]. Nevertheless, over 20,000 landfills have been cumulatively constructed nationwide, forming a substantial existing stock [7–9]. As landfill volumes continue to decline in the future, numerous sites will face the practical challenges of closure management and ecological restoration [7].

Landfill leachate, generated when precipitation runoff percolates through MSW, is a highly concentrated organic wastewater rich in organic degradation products, dissolved or suspended substances [10,11]. It exhibits extremely high chemical oxygen demand (COD), biochemical oxygen demand (BOD), and inorganic salt content, while also containing hazardous components such as organic compounds, heavy metals, and ammonia nitrogen [10]. Currently, sanitary landfills primarily rely on engineering measures such as bottom liner systems, top cover systems, and stormwater diversion to control the generation and migration of leachate [12]. However, liners are prone to aging and damage during long-term operation [13]. Once the basal liner fails, leachate may migrate downstream under hydrodynamic forces, causing groundwater contamination [14]. Such contamination not only incurs exorbitant remediation costs but also poses long-term threats to ecosystems and human health [15,16]. In addition, informal landfills, lacking leachate control facilities, present even higher groundwater contamination risks due to rainfall infiltration and surface runoff [17]. Against the backdrop of intensifying climate change and human activities, there is an urgent need for in-depth research on the spatial distribution characteristics and dynamic evolution patterns of groundwater pollutants from landfills.

The migration of landfill contamination plumes is significantly influenced by hydrogeological conditions, including site topography, stratum permeability, geological structure, and groundwater flow patterns [10,18]. These factors collectively govern plume migration through advection-dispersion processes [10,18]. Based on the hydrogeological characteristics of 80 landfills in China, Zhan et al. [19] classified them into three types: plain-type, terrace-type, and valley-type. More than 60% of China's population is distributed in plain areas with terrain slopes less than 4°, making plain-type landfills widely distributed in densely populated regions such as the North China Plain, Northeast China Plain, and the middle and lower reaches of the Yangtze River Plain, posing the greatest potential threat to public health [20,21]. Compared to other landfill types with relatively confined hydrogeological settings, plain-type sites are characterized by flat terrain, shallow groundwater levels (usually <10 m), and small hydraulic gradients (0.1‰–1‰), resulting in relatively low pollutant migration rates but wider diffusion ranges [19]. Studies based on leachate pollution indices indicate that the pollution potential of plain-type landfills is generally higher than that of other types [22]. In particular, the flat terrain and shallow groundwater

levels characteristic of these regions significantly increase the vulnerability of the aquifer. The minimal topographic gradient favors infiltration, while the proximity of the water table to the ground surface allows leachate to more easily infiltrate and reach the groundwater system, thereby escalating the risk of widespread contamination.

Furthermore, intensive human activities, high groundwater extraction rates, and climate sensitivity in plains further complicate groundwater contaminant migration mechanisms [23]. Research indicates that precipitation patterns, including interannual variability and seasonal fluctuations, as well as the increase in extreme rainfall events, can significantly alter groundwater infiltration fluxes and leachate production, thereby affecting the spatiotemporal distribution of contaminants entering the aquifer and the processes of dilution or concentration [24]. Both numerical simulations and field studies have confirmed that groundwater extraction modifies the aquifer flow field, potentially elongating or altering the direction of contaminant plumes, and in some cases accelerating contaminant migration [25]. However, most current studies focus on the impact of a single factor, such as seasonal precipitation or pumping, on contaminant transport, while there remains a lack of long-term, multi-factor research that integrates future climate scenarios with human activities [24]. Consequently, research on the migration patterns of groundwater pollution from plain-type landfills under the coupled influence of climate change and human activities remains insufficient.

The migration pathways and impact ranges of pollutants are typically determined through long-term continuous monitoring. However, due to the concealed nature and three-dimensional flow characteristics of groundwater systems, monitoring alone cannot comprehensively and accurately delineate the extent of pollution plumes [26]. Therefore, numerical simulation has become an important tool for studying the migration processes of groundwater pollutants and their long-term environmental effects [14,27]. As early as 1982, Sykes et al. [28] pioneered numerical simulations of landfill groundwater plumes to investigate contaminant migration mechanisms.

Under the strict regulatory requirements of China's Standard for Pollution Control on the Landfill Site of Municipal Solid Waste and the Zero-Waste City initiative [29], understanding the long-term evolution of legacy landfills is critical [30]. To address the complex coupling mechanisms governing contaminant plume migration under the specific dual drivers of precipitation variability (representing climate change) and agricultural groundwater extraction (representing human activities), this study selected a typical plain-type waste landfill in North China as the research object. Building upon field investigations and groundwater monitoring, a numerical model was established using the coupled MODFLOW and MT3DMS codes [31,32] to conduct coupled groundwater flow and solute transport simulations. Through the analysis of historical and future scenario simulations, this study aims to elucidate contaminant migration mechanisms under the combined effects of climate change and human activities [33], thereby providing a quantitative scientific basis for the post-closure supervision, risk assessment, and regional groundwater protection strategies required for legacy landfills in high-density plain regions.

2. Study Area

2.1. Geographical Location and Site Overview

The study area is situated in northeastern Henan Province (Figure 1a,b), within the hinterland of the Northern Henan Alluvial Plain, adjacent to the Yellow River to the east. It features a warm-temperate continental monsoon climate, with a mean annual temperature of 14.2 °C and average annual precipitation of 602 mm, concentrated predominantly from June to September. The annual evapotranspiration is approximately 530 mm.

The landfill covers a total area of 96,700 m^2 with an approximately rectangular layout, featuring a total storage capacity of 920,700 m^3 and primarily receiving municipal solid waste. Although moderate in scale, this site is highly representative of plain-type landfills widely distributed in China's county-level regions. Such sites typically share common hydrogeological characteristics, including thick Quaternary porous aquifers and shallow water tables [19,34], making the findings of this study broadly applicable to similar facilities across the North China Plain. Regarding its operational timeline, Phase I and II projects were completed in 2008 and 2009, respectively, and the site is currently closed following its designed service life. To ensure environmental safety, the landfill was constructed with a standard anti-seepage system—consisting of an HDPE geomembrane and a compacted clay liner—and a bottom leachate collection system. Nevertheless, field investigations identify villages and farmland within a 1 km radius northwest of the site as sensitive receptors for potential groundwater contamination. Finally, as illustrated in Figure 1b, several artificial channels surround the site, most notably the Wenming Canal to the southeast and its northern tributary, which constitute the primary surface water system in the study area.

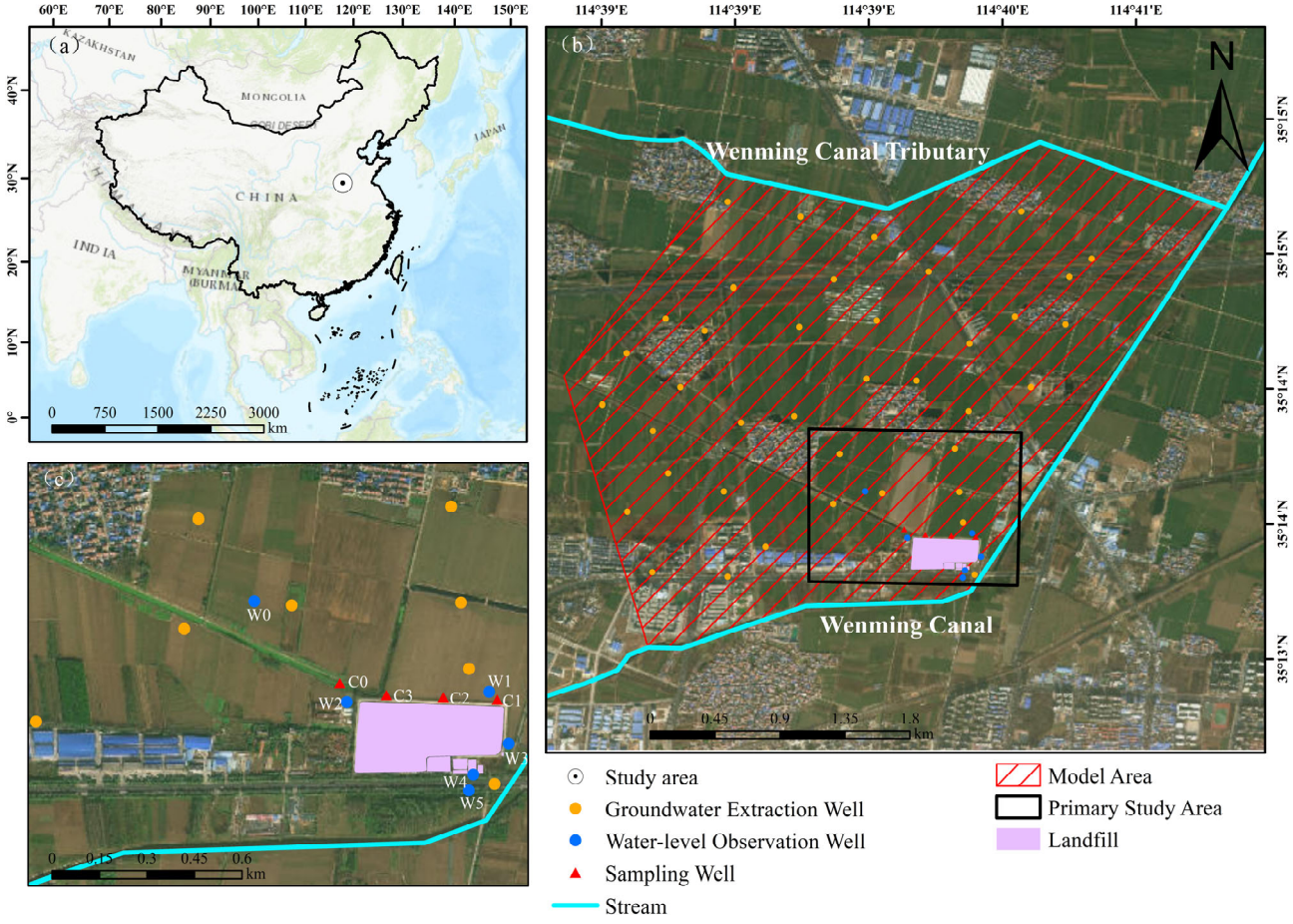


Figure 1. (**a**) Location of the study area. (**b**) Model domain and the primary study area. (**c**) Locations of the landfill, groundwater extraction wells, real monitoring wells (W1–W5 for water level, C1–C3 for chloride), and virtual observation points (W0 for water level, C0 for concentration) used in scenario analysis.

2.2. Hydrogeological Conditions

The study area lies within the Yellow River Alluvial Plain, characterized by generally flat topography with a gradual slope descending from southwest to northeast. According to unpublished regional hydrogeological data, regional groundwater occurs in Quaternary and Neogene unconsolidated sediments, which can be classified into three aquifer systems

based on burial conditions and lithology: shallow unconfined aquifer (Holocene and Upper Pleistocene), middle confined aquifer (Middle and Lower Pleistocene) and deep confined aquifer (Neogene) (Figure S1). The shallow aquifer has a thickness of 35–60 m, composed of fine sand, medium sand, and silt. It exhibits a hydraulic conductivity ranging from 4.23 to 17.32 m/d. Groundwater depth ranges from 3.4 to 5.3 m, flowing predominantly from southeast to northwest with a hydraulic gradient of approximately 1‰. The base of the shallow aquifer consists of an aquitard or weakly permeable layer of silty clay and clay. The middle and deep aquifers are confined systems [34]. Borehole data reveal that aquifers near the site consist of approximately 30 m of Quaternary alternating silt and fine sand underlain by a clay layer. In the conceptual cross-section shown in Figure 2, this silt-fine sand sequence is generalized and represented as a single "Silt" unit, reflecting the predominant matrix observed in the site-specific boreholes. The nearest channel (Wenming Canal) is located 5 m southeast of the landfill and maintains hydraulic connectivity with groundwater (Figure 1b). The Wenming Canal is an unlined earth channel, facilitating significant hydraulic interaction with the shallow groundwater. It acts as a controlling hydraulic boundary for the unconfined aquifer. Another east–west oriented channel situated 2.3 km north of the site also exhibits hydraulic connection with groundwater. Other channels show no significant hydraulic linkage to groundwater. Hydrogeologically, they act as the primary hydraulic boundaries for the study area, controlling the regional groundwater flow field and serving as sources for lateral recharge or discharge.

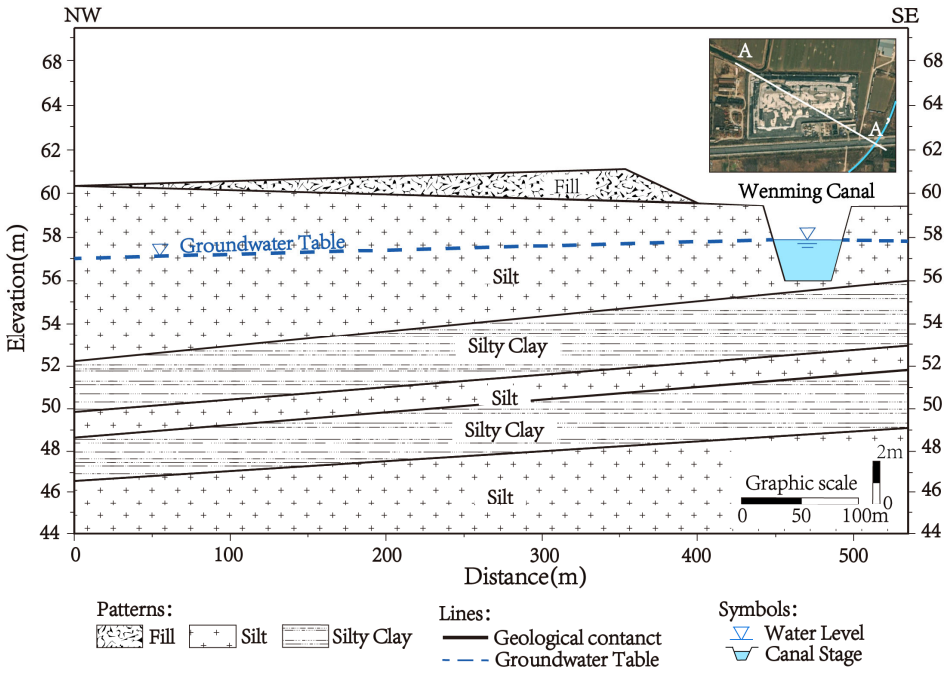


Figure 2. Conceptual hydrogeological cross-section A–A′ through the landfill site. The illustration in the upper right corner shows the location of the landfill's A–A′ section (white line), with the blue line in the diagram representing the Wenming Canal.

3. Materials and Methods

3.1. Data Sources

This study employs monthly precipitation and evapotranspiration data from the ERA5-Land reanalysis dataset as primary model inputs. ERA5 (the fifth generation ECMWF atmospheric reanalysis of the global climate) is a high-resolution global atmospheric reanalysis dataset developed and maintained by the European Centre for Medium-Range Weather Forecasts (ECMWF). It provides continuous, consistent, and high-quality data se-

ries for multiple meteorological and climate variables. The ERA5 series primarily includes two products: ERA5 (global coverage) and ERA5-Land (land-focused). Comparatively, ERA5-Land offers higher spatial resolution (up to 0.1°) versus ERA5's maximum resolution of 0.25°. Both datasets are widely employed in hydrological research [35,36].

Information on the geology and hydrogeology of the study area—necessary for determining the aquifer characteristics (e.g., aquifer thickness) and hydraulic parameters (e.g., hydraulic conductivity, specific yield)—was obtained from the report of Investigation and Assessment of Groundwater Environmental Conditions in Landfill Sites of Henan Province. The river level data utilized to define the model boundary conditions were obtained through on-site field surveys. Since the Wenming Canal and its tributary are artificial channels with controlled flow regimes, their water levels remain relatively stable with minimal seasonal fluctuation, making the field-measured values representative for the simulation period. Groundwater extraction data were based on field survey data from local agricultural departments regarding irrigation practices.

Additional groundwater data were exclusively collected through field monitoring around the landfill site (Figure 1c). Specifically, groundwater level data originated from five monitoring wells (W1W5) installed upstream, downstream, and laterally around the site (Text S1 and Table S3), with measurements recorded in August 2023. Since the regional groundwater flows from southeast to northwest, the monitoring wells were strategically installed along the northern and northwestern boundaries (the downstream direction) to effectively capture the migration of the contaminant plume.

Solute concentration data were acquired from three downstream monitoring points (C1, C2, C3) during sampling campaigns in November 2020, July 2022, and October 2022. To comprehensively evaluate the site's contamination status, a suite of hydrochemical parameters was analyzed, including chloride (Cl^-), manganese (Mn^{2+}), nitrate (NO^{3-}), sulfate ($SO_4{}^{2-}$), total dissolved solids (TDS), and total hardness. All water samples were collected and preserved in accordance with standard technical specifications. The laboratory analysis was performed by the Henan Rock and Mineral Testing Center (CMA-accredited). Specifically, major anions such as chloride, nitrate, and sulfate were determined using a Dionex AQUION IC ion chromatograph (Thermo Fisher Scientific, Waltham, MA, USA), while other parameters were measured following the national Standard Methods for the Examination of Water and Wastewater.

3.2. Methodological Approach

This study developed a coupled, transient numerical model for groundwater flow and solute transport using the MODFLOW (version 2005) and MT3DMS (version 5.3) codes within the GMS software (version 10.0, Aquaveo, Provo, UT, USA). Given the relatively thin aquifer thickness (30~40 m) compared to the lateral extent and the homogeneous lithology of the alluvial plain, the shallow aquifer was generalized as a single layer [37–39]. To evaluate the effectiveness of model parameter calibration and the accuracy of the simulation, indicators such as Mean Error (ME), Mean Absolute Error (MAE), and Root Mean Square Error ($RMSE$) were employed to assess the model's performance in simulating water levels and concentrations. Their calculation formulas are as follows:

$$ME = \frac{1}{n}\sum_{i=1}^{n}(\hat{y}_i - y_i)$$

$$MAE = \frac{1}{n}\sum_{i=1}^{n}|y_i - \hat{y}_i|$$

$$RMSE = \sqrt{\frac{1}{n}\sum_{i=1}^{n}(y_i - \hat{y}_i)^2}$$

where n is the total number of observations, y_i represents the i-th measured values of certain variables (water levels or chloride concentrations), and $\hat{y}_i$ represents the i-th simulated value. The simulation period covers historical conditions (2021–2025) and future projections (2025–2040). Chloride (Cl^-) was selected as a conservative tracer to simulate the contaminant plume migration. Based on this coupled framework and validated model, several scenarios were simulated to evaluate the impacts of precipitation changes and groundwater extraction intensity on plume evolution (Figure 3).

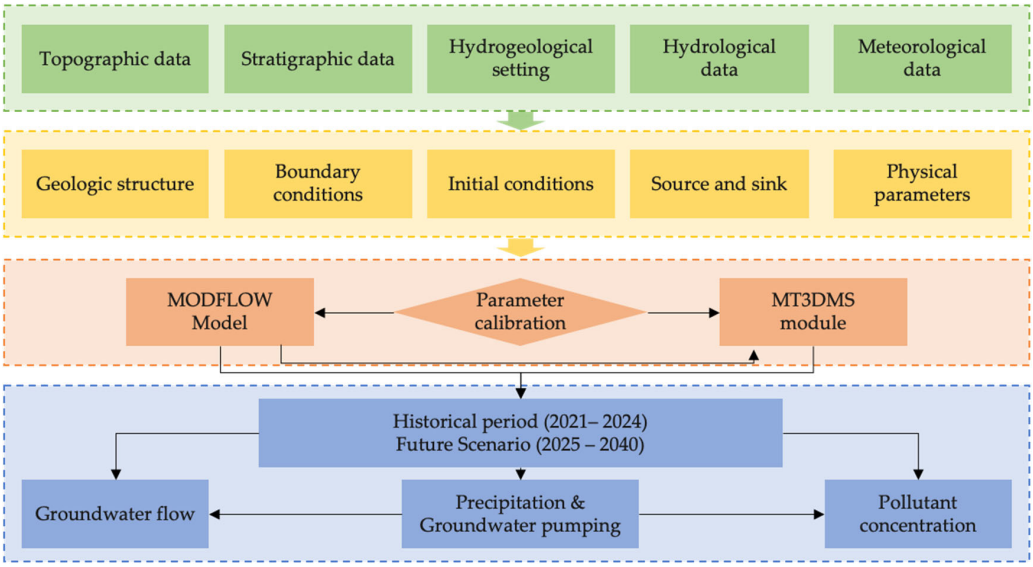


Figure 3. Technical roadmap of this study. Colors represent different workflow phases: data acquisition (green), model setup (yellow), simulation (orange), and scenario analysis (blue).

3.3. Model Development Procedure

3.3.1. Groundwater Flow Model

According to borehole data, the shallow aquifer with a thickness of 40 m, composed of fine sand, medium sand, and silt, was generalized as a single-layer aquifer. Spatial discretization adopted a grid resolution of 25 m in both east–west and north–south directions, totaling 21158 model cells. Temporally, the simulation period was divided into two phases: 20212025 as the historical period and 2025–2040 as the future projection period. Monthly stress periods and daily computational time steps were implemented throughout the simulation.

Based on the hydrogeological conditions of the study area and the hydraulic connections between surface water and groundwater, the model domain was delineated with the main channel of Wenming Canal as the southeastern boundary and its tributary as the northern boundary. Reflecting their dominant control on the flow field, both boundaries were designated as specified-head boundaries, with head elevations set to 5 m below the local ground surface elevation, based on annual average river water levels. Given the flat terrain and characteristic perpendicular groundwater flow direction near river channels in this region, the western boundary was established perpendicular to both channels and assigned as a no-flow boundary.

The initial conditions for the transient simulation (January 2021) were established by running the model to a steady-state condition. This “spin-up” phase used long-term average recharge and boundary conditions to generate a stable flow field, which was

aligned with the observed regional groundwater depth of 3–4 m and subsequently used as the starting head for the historical simulation.

The study area is characterized by flat terrain and a shallow groundwater table. The primary source of groundwater recharge is precipitation infiltration, while discharge occurs mainly through phreatic evaporation and groundwater extraction. Given the relatively small size of the simulation area and the simplicity of the underlying surface types, surface runoff was neglected in this study. The net groundwater recharge (R) for each stress period was derived by subtracting the actual evapotranspiration (E_{actual}) from the total precipitation (P):

$$R = P - E_{actual}$$

Both monthly precipitation and actual evapotranspiration data were obtained from the ERA5-Land reanalysis dataset. This approach accounts for surface evaporation and plant transpiration losses, providing a more realistic estimation of the infiltration flux entering the aquifer.

According to field survey data, the average groundwater extraction intensity in the study area is 40×10^4 $m^3/(km^2 \cdot a)$. In accordance with local agricultural irrigation practices, the annual groundwater extraction wells (Figure 1b) in the study area are screened in the shallow aquifer (depths of 20–50 m) and were simulated using the Well (WEL) package in MODFLOW. The pumping regime follows the local agricultural cycle: 40% from March to May (spring irrigation), 40% from June to August (summer irrigation), and the remaining 20% over the other six months of the year.

Based on the results of pumping tests and borehole lithology tests conducted in the study area, initial ranges for the model's hydraulic conductivity and specific yield parameters were established. The aquifer was assumed to be homogeneous, with parameter values (as listed in Table 1) applied uniformly across the model domain.

Table 1. Hydrogeological parameters.

Parameter	Value
Horizontal Hydraulic Conductivity (m/d)	5
Vertical Hydraulic Conductivity (m/d)	0.5
Specific Yield (-)	0.20
Effective Porosity (-)	0.25
Longitudinal Dispersivity (m)	30
Transverse Dispersivity Ratio (-)	0.25
Vertical Dispersivity Ratio (-)	0.10

3.3.2. Solute Transport Model

Based on sampling analyses from seven monitoring points around the landfill site, the primary contaminants surpassing standards in groundwater include chloride, manganese ions, nitrate, sulfate, total hardness, and total dissolved solids, with maximum magnitudes of non-compliance of 2.37, 1.22, 1.57, 1.19, 1.87, and 0.80 times the limit, respectively. Among these, chloride levels were found above the threshold at four locations, with average concentrations more than doubling the permissible limit, establishing it as a major groundwater contaminant in the area. Given chloride's characteristics—high solubility, strong mobility, low degradability, and minimal plant uptake—it effectively indicates contamination plume migration. Therefore, chloride was selected as the tracer element for this study. While the leachate contains significant degradable organic pollutants, modeling them requires complex decay parameters that are site-specific and currently unavailable [18,33]. More importantly, from a risk assessment perspective, organic pollutants migrate slower than chloride due to biodegradation and adsorption [10,18,33]. Consequently, chloride serves

as a conservative proxy: its migration plume defines the maximum physical envelope of groundwater contamination [33]. Any area unaffected by the chloride plume can be considered safe from the less mobile organic contaminants.

Given that the reactions between chloride ions and the surrounding environment during migration are relatively limited, this study primarily considered the processes of advection and dispersion. The parameters for contaminant migration, particularly effective porosity and dispersivities, were initially estimated from literature and subsequently refined through rigorous manual calibration to match the observed spatial distribution and arrival times of the chloride plume. The initial chloride concentration for the entire model domain as of January 2021 was set to 30 mg/L. This value was based on monitoring data from upstream and peripheral wells (e.g., C1, C2, C3 in November 2020, as shown in Table 2), representing the background concentration before significant plume migration.

Table 2. Comparison of observed and simulated chloride concentrations (unit: mg/L).

Monitoring Well	Time	Observed	Simulated
C1	2020/11	29	30
C1	2022/7	47	51
C1	2022/10	64	58
C2	2020/11	33	30
C2	2022/7	66	62
C2	2022/10	54	69
C3	2020/11	24	30
C3	2022/7	53	54
C3	2022/10	57	61
Overall performance	ME = 2.0	MAE = 4.6	RMSE = 6.24

The landfill leachate source was defined as a specified concentration associated with the recharge flux applied to the entire landfill footprint (total area of 96,700 m^2). Specifically, the chloride concentration was fixed at 2000 mg/L throughout the simulation period. Although recent field sampling indicated a lower instantaneous concentration (572 mg/L), downstream monitoring wells recorded chloride levels exceeding 1100 mg/L, suggesting historically higher leakage concentrations. Furthermore, this value aligns with the typical range (1500–4000 mg/L) reported for municipal solid waste leachate in North China [5,11], serving as a conservative source term to prevent the underestimation of long-term contamination risks. This setting represents a conservative, 'worst-case' scenario, assuming sustained high-concentration leakage without temporal decay.

3.3.3. Model Calibration and Validation

Based on the observed groundwater level and chloride concentration data, combined with existing hydrogeological data and relevant field test results, the hydraulic conductivity, effective porosity, and dispersivity of the historical period (2021–2024) model were calibrated using the observed groundwater level and chloride concentration data. By carefully adjusting these parameters, the model was able to simultaneously capture the hydrodynamic flow field and the solute transport dynamics.

To assess the reliability of the model, the simulated groundwater levels and chloride concentrations were compared with measured data. Water level validation utilized August 2023 data from five monitoring wells (W1–W5), showing differences between simulated and observed values ranging from 0.2 to 0.9 m (Figure 4a, Table 3), with the ME, MAE, and RMSE being −0.12 m, 0.5 m, and 0.59 m, respectively. Concentration validation employed measured data from wells C1–C3 during November 2020, July 2022, and October 2022. The

model yielded a ME of 2.0 mg/L, a MAE of 4.6 mg/L, and a RMSE of 6.24 mg/L, with consistent trend alignment between simulations and observations (Figure 4b, Table 2).

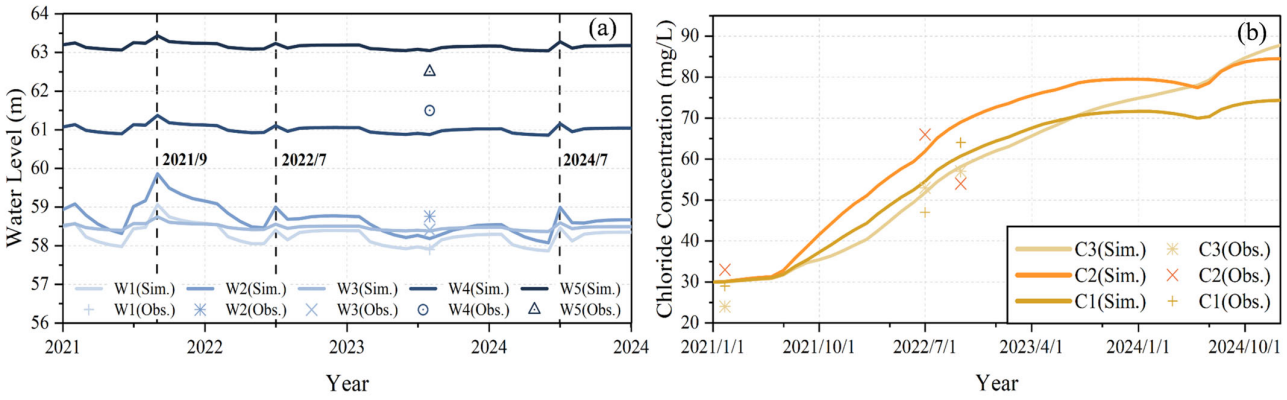


Figure 4. (**a**) Simulation results of historical water levels; (**b**) simulation results of historical chloride concentrations.

Table 3. Comparison of observed and simulated water levels (unit: m).

Monitoring Well	Time	Observed	Simulated
W1	2023/8	58.8	58.5
W2	2023/8	58.0	57.1
W3	2023/8	58.4	58.6
W4	2023/8	61.5	61.1
W5	2023/8	62.5	63.3
Overall performance	ME = −0.12	MAE = 0.52	RMSE = 0.59

It is important to address the representativeness of the monitoring network. Although the number of observation wells (n = 5) is limited, their spatial distribution is strategically aligned with the regional hydrogeological boundaries: wells W4 and W5 capture the upstream inflow, W1 monitors the lateral boundary, and W2 and W3 control the downstream outflow. Given the relatively homogeneous lithology of the alluvial plain aquifer, this spatial configuration effectively constrains the regional hydraulic gradient [19,34]. The satisfactory calibration results (RMSE = 0.59 m for head and 6.24 mg/L for concentration) further confirm that the current dataset is adequate to support the simulation of macro-scale plume evolution trends. These results demonstrate satisfactory performance in simulating both groundwater flow fields and solute transport, reliably reflecting the hydrogeological characteristics of the study area and meeting requirements for subsequent scenario predictions.

3.4. Model Scenario Settings

Taking into account the impacts of precipitation changes and groundwater extraction intensity, multiple future scenarios are designed as model inputs to simulate the evolution processes of groundwater levels and solute concentrations over the next 15 years (from January 2025 to December 2040). This timeframe was selected to align with the regional "2035 Long-Range Planning" horizon, balancing prediction relevance with the uncertainties of long-term socio-economic forecasting. In these scenarios, "human activities" are specifically represented by groundwater extraction intensities, which are inversely coupled with precipitation to reflect agricultural irrigation demand. Specifically, this analysis focuses on quantifying the spatiotemporal dynamics of the contaminant plume driven by the coupled

stresses of precipitation variability (climate change) and groundwater extraction intensity (human activities).

The future scenario settings primarily consider the joint impacts of climate change (precipitation changes) and human activities (groundwater extraction) on groundwater flow fields and pollutant migration. Since groundwater in the study area is mainly used for agricultural irrigation, changes in precipitation directly affect irrigation demand and groundwater stress. Therefore, in the scenario assumptions of this study, a decrease in precipitation corresponds to enhanced groundwater extraction, and vice versa.

Regarding the degree of climate change, the commonly used approach is to adopt CMIP6-based SSP scenario projections; however, such datasets are generally suitable for large-scale modeling and have limited applicability at the site scale. Accordingly, this study empirically defined five scenarios based on local long-term precipitation variability, irrigation demand, and the safe yield of the aquifer: a high-precipitation scenario (+20%) with no irrigation demand (S1), a low-precipitation scenario (-10%) representing the maximum permissible groundwater withdrawal (S4), two intermediate scenarios with $\pm 5\%$ changes in precipitation (S2/S3), and a baseline scenario maintaining current conditions (S0). Then, monthly precipitation distributions were allocated proportionally under each annual scenario. Specifically, the baseline extraction rate (S0) was set at 40×10^4 $m^3/(km^2 \cdot a)$ based on current survey data. For the high-precipitation scenario (S1, +20% rainfall), groundwater extraction was set to 0, assuming rainfall meets all irrigation needs. Conversely, for the low-precipitation scenario (S4, -10% rainfall), extraction was increased to 60×10^4 $m^3/(km^2 \cdot a)$, representing a high-stress condition driven by drought. Although potential changes in land use or water-use structure were not considered, these scenarios capture two opposite extremes of precipitation and groundwater extraction. This setup is believed to provide valuable insights for groundwater management (Table 4).

Table 4. Future scenario settings for the model.

Scenarios	Mean Annual Precipitation (mm)	Annual Pumping Intensity (10^4 $m^3/km^2 \cdot a$)
S0	640	40
S1	768 (640 +20%)	0
S2	704 (640 + 5%)	30
S3	608 (640 − 5%)	50
S4	576 (640 − 10%)	60

4. Results

4.1. Characteristics of Groundwater Flow Fields and Pollutant Migration in Historical Simulation Periods

The simulation results from 2021 to 2025 reveal that the groundwater flow field in the study area generally exhibits a migration trend from southeast to northwest (Figure 5a), primarily controlled by surface water recharge from the Wenming Canal and topographic gradients. As explicitly identified in Figure 5a, the primary groundwater flow path originates from the southeastern boundary (recharged by the canal) and migrates towards the northwest. Additionally, influenced by seasonal variations in precipitation and groundwater extraction intensity, the water levels display significant dynamic fluctuations, typically reaching their peak during the flood season (July–September) and gradually declining during the dry season (Figure 4a). Notably, during the high-extraction periods for agricultural irrigation (March–May and June–August), the decline in water levels leads to a steepening of the local hydraulic gradient. This seasonal hydrodynamic shift temporarily accelerates

groundwater flow velocity, thereby enhancing the advective transport of the contaminant plume towards the northwest.

Driven by this flow regime, the chloride concentrations in monitoring wells C1, C2, and C3 consistently increased over the five-year period, indicating that the front of the pollutant plume had gradually migrated to these monitoring points (Figure 5b). As shown in the spatial distribution, a distinct plume accumulation is observed at the northwestern boundary. This phenomenon is governed by coupled engineering and hydrodynamic factors: the landfill's anti-seepage system acts as a physical barrier that initially confines the leachate pool. Simultaneously, the predominant southeast-to-northwest groundwater flow transports contaminants leaching from the upstream sector to the downstream edge. In this northwestern corner, the transported upstream load superimposes with local leakage, forming a high-concentration zone before dispersing further downgradient. Specifically, from the beginning of 2021 to the end of 2025, the simulated chloride concentrations in all three wells exhibited an upward trend. By the end of this period, the concentration in well C3 rose from 30.0 mg/L to 87.6 mg/L, in well C2 from 30.0 mg/L to 84.9 mg/L, and in well C1 from 30.0 mg/L to 74.3 mg/L (Figure 4b). While well C2 initially showed the highest concentration during 2022 (consistent with the observations in Table 2), the sustained transport of the contaminant plume caused well C3 to eventually become the highest by late 2024. This persistent concentration gradient (C3 > C2 > C1) observed at the end of the historical period aligns with the plume distribution in December 2024 (Figure 5b), indicating that the primary migration pathway aligns closest to Well C3's position.

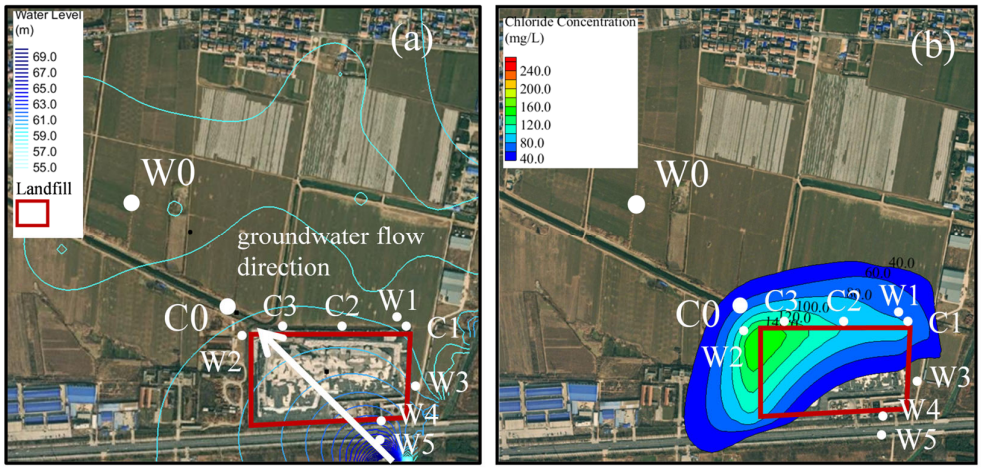


Figure 5. (**a**) Groundwater flow field in the primary study area (the white arrow indicates the direction of groundwater flow). (**b**) Distribution of contaminant plume in the primary study area at the end of the historical simulation period (December 2024).

4.2. Dynamic Characteristics of Groundwater Contamination Plumes Under Future Scenarios

4.2.1. Response of Groundwater Levels to Scenarios

To evaluate the impacts of different combinations of climate and human activity scenarios on the groundwater system, a water level observation point W0 was established along the groundwater flow direction, between the landfill site and the village (Figure 5). Based on the simulation results from 2021 to 2040, the dynamic changes in water levels at W0 under different scenarios were analyzed (Figure 6).

Throughout the simulation period, the groundwater level at W0 exhibited distinct seasonal fluctuations. Within a year, the water level declined in the first half of the year and rose in the second half, influenced by groundwater extraction, with the lowest level typically occurring in June or July and the highest level from September to November.

Long-term trends showed clear divergence among scenarios, with differences becoming increasingly pronounced over time.

Analysis of W0 water level data revealed the following average level hierarchy (Table S2): S1 (58.6 m) > S2 (58.4 m) > S0 (58.3 m) > S3 (57.9 m) > S4 (57.6 m). High-pressure (S3) and extreme-pressure (S4) scenarios caused significant water level declines, with S4 yielding the lowest average level (57.6 m), consistent with expected storage depletion from reduced precipitation and increased extraction.

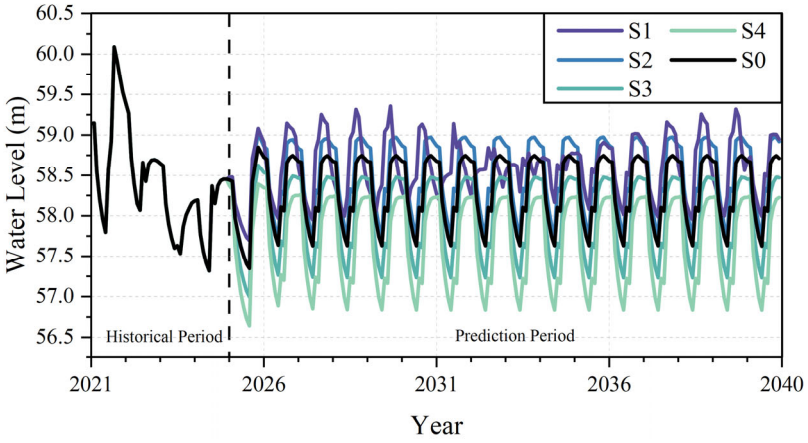


Figure 6. Water levels at observation point W0 under different scenarios.

4.2.2. Temporal Variation Characteristics of Pollutant Concentrations

The spatiotemporal evolution of pollutant concentration exhibits significant differences under various scenarios. The C1 monitoring well, located at the edge of the landfill (Figure 5), reflects the concentration variation characteristics in the core area of the pollution plume (Figure 7a). The results indicate that the pollutant concentration continues to rise under all scenarios. It is crucial to distinguish that precipitation drives the net infiltration rate entering the aquifer. Since this study focuses on regional groundwater transport and does not explicitly simulate complex partition processes (e.g., adsorption or retardation) within the vadose zone, the infiltration flux essentially acts as the carrier for contaminant input. Consequently, the impact of infiltration rate exhibits scale-dependent characteristics: on a seasonal scale, intense rainfall events may lead to temporary concentration dilution; Over time, the growth in concentration gradually slows down: before 2030, the concentration changes approximate a linear increase, while the timing of the concentration inflection point is delayed as precipitation increases.

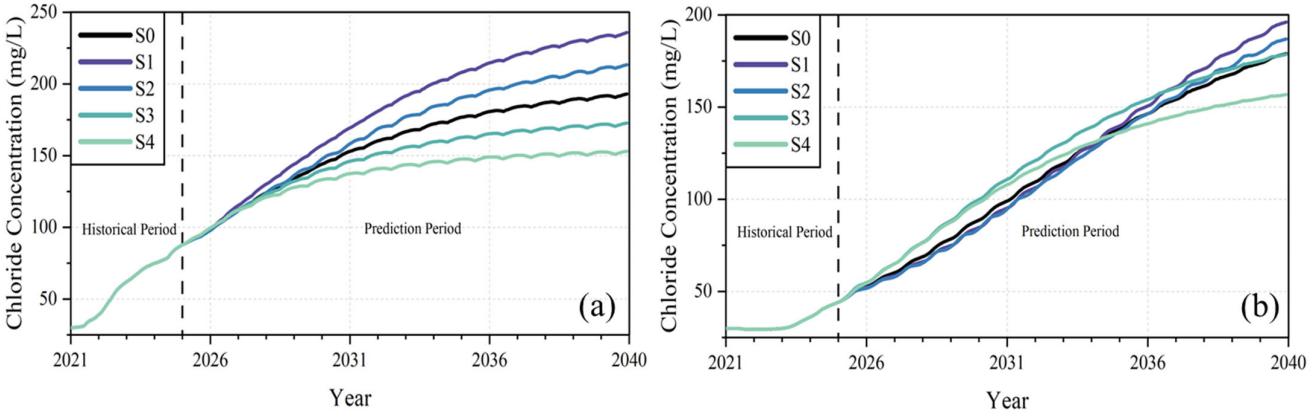


Figure 7. (**a**) Chloride concentrations at monitoring well C1 under different scenarios; (**b**) chloride concentrations at observation point C0 under different scenarios. The vertical dashed line separates the historical simulation period from the future prediction period.

To characterize the downstream propagation of the contaminant plume, the temporal evolution of chloride concentrations was analyzed at observation point C0 (Figure 7b), located along the primary groundwater flow path (Figure 5). Unlike C1, under low-precipitation scenarios (S3 and S4), C0 shows rapid plume advancement and steep concentration rises before 2035, followed by slowed increases. Conversely, under high-precipitation scenarios (S1 and S2), initial migration at C0 is slower with delayed concentration increases, yet maintains relatively stable growth rates. Notably, post-2035 concentrations in S1/S2 overtake those in S3/S4. This crossover phenomenon provides a clearer picture of the dual-driver mechanism: while increased hydraulic gradients from intensified extraction (S3, S4) accelerate the initial arrival of the plume front, the increased annual infiltration in S1 and S2 significantly enhances the leaching intensity within the landfill body. This higher infiltration flux acts as a more efficient carrier, delivering a substantially greater total mass flux of chloride to the aquifer over the long term, eventually resulting in higher concentration peaks at the downstream receptor despite the slower advective velocity. The distinct temporal trends at these locations are governed by their spatial proximity to the source. The concentration at monitoring well C1, located at the immediate edge of the landfill, tends to stabilize (plateau) in the later stages as it approaches equilibrium with the continuous contaminant leakage. In contrast, observation point C0 is situated downstream at the advancing front of the plume. Consequently, its concentration exhibits a continuous upward trend as the contaminant plume expands and the high-concentration core gradually migrates towards this downstream location.

4.2.3. Spatial Evolution Characteristics of Landfill Contamination Plumes

According to the Groundwater Quality Standard of the People's Republic of China (GB/T 14848–2017) [40], the chloride concentration limits for Class I (suitable for all uses) and Class III (suitable for centralized drinking water sources and industrial/agricultural uses) groundwater are $\leq$50 mg/L and $\leq$250 mg/L, respectively. To assess the spatiotemporal evolution and potential risks of the contaminant plume, and considering possible uncertainties in model simulation, the areas enclosed by the 30 mg/L and 200 mg/L chloride concentration contours were conservatively defined as the potential impact zone and high-risk zone, respectively (Table 5).

Table 5. Temporal evolution of high-risk and potential impact zones.

Scenarios	Area of the High-Risk Zone (10^3 m^2)			Area of the Potential Impact Zone (10^5 m^2)				Leading-Edge Diffusion Distance (m)			
	2030	2035	2040	2025	2030	2035	2040	2025	2030	2035	2040
S0	-	4.49	9.91	1.52	2.15	2.40	3.66	334	384	420	452
S1	4.05	12.80	25.00	1.52	2.29	2.57	3.04	334	369	396	429
S2	2.59	9.70	16.70	1.52	2.36	2.25	2.79	334	365	392	417
S3	-	1.45	4.78	1.52	2.36	3.59	3.79	334	411	450	532
S4	-	-	-	1.52	2.47	3.19	4.16	334	422	480	549

Comparative analysis of simulation scenarios reveals that the emergence timing of high-risk groundwater contamination zones advances or delays with increasing or decreasing precipitation, while their areas gradually expand over time. Under S1 and S2 scenarios, high-risk zones appear before 2030; under S0 and S3 scenarios, they emerge by 2035; whereas no high-risk zone is detected by 2040 under S4. Figure 8 shows that under baseline conditions (S0), the high-risk zone is projected to extend beyond site boundaries by 2037, posing potential threats to surrounding environments.

In contrast to the high-risk zone, the potential impact zone of the pollutant plume exhibits an opposite pattern of change. Both the area of the impact zone and the leading-edge diffusion distance (Table 5) demonstrate that the greater the intensity of groundwater

extraction (i.e., the less precipitation), the faster and more extensive the diffusion of pollutants. By 2040, the S4 scenario exhibits the maximum leading-edge diffusion distance (549 m) and the broadest impact zone (4.16×10^5 m^2), while the S1 scenario, which involves no extraction, shows minimal values for both indicators. These spatial evolution characteristics, as visualized in Figure 8 and summarized in Table 5, underscore two principal findings of the scenario analysis. First, increased recharge (Scenarios S1 and S2) causes the contamination plume to expand notably toward the east and south, likely due to the localized mounding effect of the water table under high-precipitation conditions. Second, intensified groundwater extraction (Scenarios S3 and S4) results in higher groundwater flow velocities by steepening the regional hydraulic gradient, which subsequently leads to substantially greater plume migration distances toward the northwest. These mechanisms demonstrate that while precipitation primarily influences the lateral expansion and core concentration, extraction intensity is the dominant driver for the longitudinal advancement of the plume.

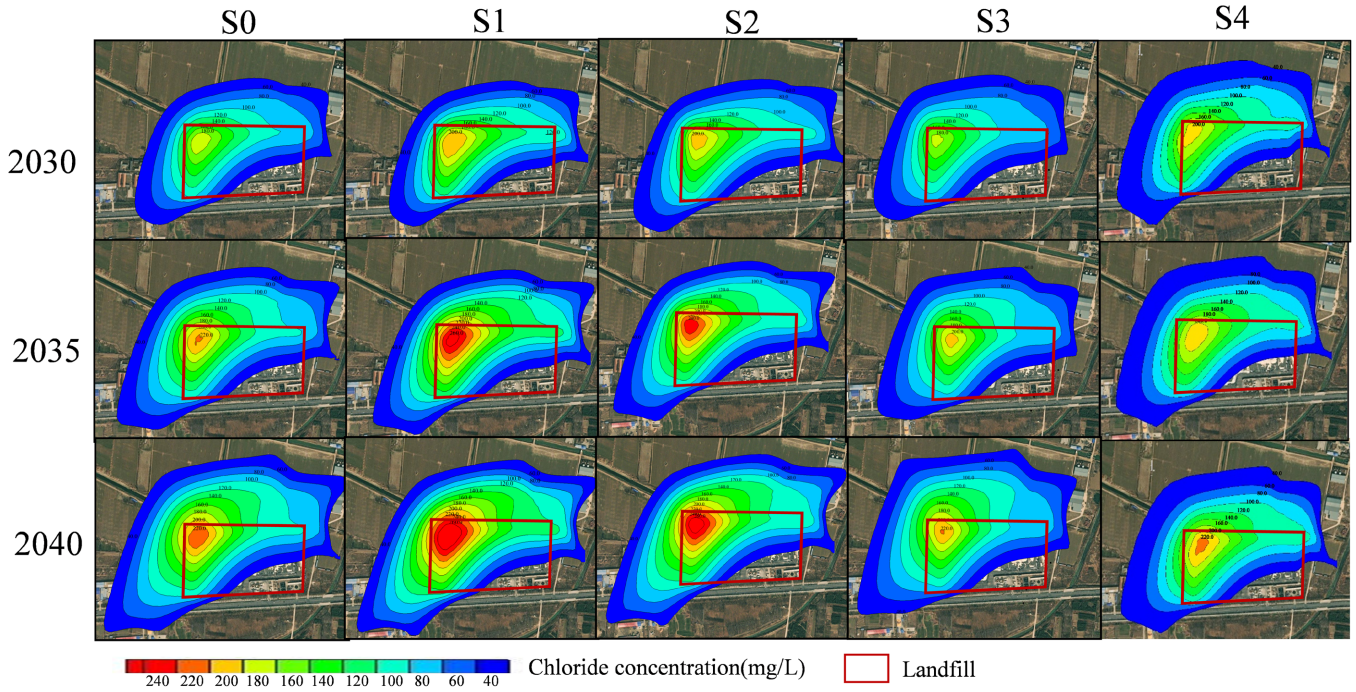


Figure 8. Characteristics of contaminant plumes under different scenarios.

5. Discussion

5.1. Impacts of Precipitation Changes and Groundwater Exploitation on the Migration of Groundwater Contaminants at Landfills

Climate change has significantly altered precipitation patterns in many regions, manifesting as variations in annual precipitation totals and increased frequency of extreme rainfall events. These changes have emerged as critical climatic drivers affecting groundwater contaminant transport from landfills [24,41]. The simulations reveal substantially higher contaminant concentrations in the central plume area under precipitation-increase scenarios (S1, S2) compared to precipitation-decrease scenarios (S3, S4) (Figure 8). This indicates that increased annual rainfall and storm frequency enhance infiltration fluxes through cover layers, thereby elevating leachate production rates and intensifying its pulsating characteristics. Consequently, these changes accelerate contaminant breakthrough times to aquifers [42–44]. However, at the monthly scale, concentrations decrease during high-rainfall months (Figure 7), demonstrating precipitation's dilution effect on contaminants over short-term periods. Conversely, long-term precipitation primarily drives contam-

inant transport through leaching mechanisms. Additionally, studies have shown that short-duration intense rainfall increases leachate volumes and hydraulic head, which facilitates the rapid penetration of contaminants into groundwater systems and generates transient high-concentration peaks [43,45]. Notably, under scenarios with increased precipitation, the contamination plume expands eastward and southward (Figure 8). This shift is likely attributable to reduced hydraulic gradients between surface water bodies and groundwater, which in turn elevates the risk of contaminant discharge into surface waters. Additionally, precipitation variations can modify contaminant mobility and bioavailability by altering vadose zone moisture status and redox conditions, thereby influencing metal dissolution/adsorption equilibria and organic degradation rates [46].

Meanwhile, groundwater extraction induced by human activities has become a major driver altering contaminant migration pathways and velocities. Persistent pumping causes regional water table declines and hydraulic gradient reversals, accelerating the convergence of leachate plumes toward extraction wells and elevating contamination risks in water supply systems [47]. Groundwater extraction and precipitation changes exhibit significant coupling effects [48]. The simulated scenarios ("precipitation increase + extraction reduction" vs. "precipitation decrease + extraction intensification") demonstrate that increased pumping rates enhance SE–NW hydraulic gradients (Table 5), accelerating flow velocities and significantly expanding plume migration distances. This evidences complex nonlinear amplification effects between precipitation variation and groundwater extraction [24,47]. Identifying this primary flow path is critical for regulatory decision-making. It enables the transition from blanket monitoring to targeted supervision, guiding the cost-effective placement of early-warning wells along the advective axis and delineating precise downstream "restricted extraction zones" to meet compliance standards.

The dual drivers of climate change and human activities suggest that landfill contamination plumes may expand further under future environmental changes. Existing liner systems and leachate collection infrastructure offer inadequate long-term protection for groundwater security. Post-management of landfills will require enhanced high-frequency monitoring of groundwater levels and quality over a broader range, the establishment of risk early warning systems, and the formulation of dynamic control measures [45,49].

5.2. Research Uncertainties and Future Prospects

This study conducted a systematic analysis of the spatial distribution and future evolution trends of groundwater pollution plumes at landfills through a combination of field investigations, sampling analysis, and groundwater numerical simulations, offering valuable insights into the potential expansion paths and risks of pollution plumes under changing environmental conditions. However, several uncertainties and limitations persist, necessitating further refinement in subsequent research.

Current groundwater management in the region is severely constrained by the lack of systematic monitoring infrastructure. The dataset used in this study, while capturing the primary migration trends through three sampling campaigns (2020–2022), represents the limited data availability typical of such developing regions. This data scarcity underscores the urgency of this research: effectively utilizing available discrete data to predict potential risks is a necessary first step to inform policy. While the model calibration based on these campaigns has satisfactorily reproduced the plume evolution (RMSE = 6.24 mg/L), the establishment of a real-time, high-frequency groundwater monitoring network remains a critical priority for future validation and early warning systems.

To maximize the prediction of potential contaminant migration distances, this study selected chloride ions, which exhibit strong conservatism, as the indicator for pollution plumes, but did not incorporate the degradation, adsorption, and redox reactions of organic

pollutants and metal ions in leachate during their migration processes. This may lead to overly conservative simulation results regarding the extent and concentration of pollution.

The future scenario settings only considered two key driving factors: precipitation changes and groundwater exploitation, and the specific parameter settings inevitably involve a certain degree of subjectivity, failing to fully reflect potential impacts such as population mobility, land use changes, and regional economic development plans. Subsequent research should integrate actual socio-economic and climatic scenarios to construct more refined, multi-scenario simulation schemes and iterate and validate models through long-term monitoring data to enhance the prediction accuracy and decision-support capabilities regarding groundwater pollution risks.

Despite these limitations, the modeling framework established in this study is highly transferable. It is specifically suitable for the risk assessment of plain-type landfills widely distributed across the North China Plain and other East Asian monsoon regions. These sites share critical commonalities—porous alluvial aquifers, shallow water tables, and dual sensitivity to monsoon rainfall and agricultural pumping—making the coupled driver mechanism identified here a theoretical benchmark for regional environmental management. Moreover, these estimation-based scenarios provide a scientifically representative basis for risk assessment. The definition of end-member scenarios—ranging from the high-stress drought condition (S4) to the recharge-dominated wet condition (S1)—effectively "brackets" the potential range of future hydrological stresses. Furthermore, since the model has been rigorously calibrated against historical data (RMSE = 0.59 m), it accurately captures the aquifer's physical response mechanisms to these stresses. Therefore, even if absolute long-term predictions carry uncertainty, the model validly reflects the relative changes in risk levels under different environmental trajectories, offering valuable bounds for decision-making.

5.3. Implications for Groundwater Protection and Management

Based on the simulation results and the dual-driver mechanism identified, this study proposes specific regional groundwater pollution prevention and control strategies. Source-focused measures should prioritize the regular integrity testing of liner systems and the deployment of hydraulic containment wells immediately downstream during high-precipitation periods to intercept the enhanced vertical leaching flux. Simultaneously, plume control strategies should involve strict regulations on shallow aquifer extraction in the downstream northwest region during critical irrigation seasons (March-May) to curb the horizontal expansion caused by steepened hydraulic gradients, recommending a substitution with deep aquifer resources or diverted surface water.

More specifically, to effectively support China's Standard for Pollution Control on the Landfill Site of Municipal Solid Waste and the Zero-Waste City initiative, this study proposes a concrete regulatory roadmap based on the "dual-driver" findings. Initially, regulators should utilize the simulated typical contour lines (e.g., 30 mg/L and 200 mg/L for chloride) to establish precise "compliance boundaries" beyond the physical site, replacing vague buffer zones with scientifically delineated risk areas. Building on this zoning, a dynamic source control strategy should be prioritized during the monsoon season (June–September) by implementing hydraulic containment measures immediately downstream to intercept precipitation-driven vertical leakage spikes. Simultaneously, to curb the extraction-driven plume expansion, a strict "Restricted Extraction Zone" should be enforced in the downstream northwestern sector during critical irrigation months (March–May), substituting shallow groundwater use with deep aquifer or surface water resources.

This integrated approach shifts post-closure management from passive monitoring to active, scenario-based risk control, ensuring long-term environmental safety in high-density agricultural regions.

6. Conclusions

This study systematically investigated the spatiotemporal evolution of groundwater contamination in a representative plain-type landfill in North China through an integrated approach consisting of field investigations and numerical modeling. A coupled groundwater flow and solute transport model was developed and rigorously calibrated using field-measured groundwater levels and chloride concentration data, demonstrating robust performance in reflecting the historical hydrogeological conditions. This calibrated model was subsequently employed for scenario projections (2025–2040) to quantitatively evaluate the individual and coupled impacts of climate change (represented by precipitation variability) and human activities (represented by groundwater extraction intensity) on plume evolution.

The results elucidate a "dual-driver" coupling mechanism governing contaminant migration in semi-humid agricultural regions. It was found that precipitation variability primarily drives the vertical leaching intensity, while groundwater extraction intensity dominates the horizontal hydraulic gradient and the spatial expansion of the contamination plume. This distinction provides a theoretical basis for identifying contrasting spatial patterns under different environmental stresses. Furthermore, the validated "Investigation–Monitoring–Simulation–Prediction" framework offers a transferable and cost-effective tool for the post-closure supervision and risk assessment of legacy landfills, particularly in data-scarce plain regions.

Supplementary Materials: The following supporting information can be downloaded at: https://www.mdpi.com/article/10.3390/hydrology13010036/s1, Table S1: Monthly average precipitation and evapotranspiration in the study area from 2021 to 2024; Table S2: Statistical characteristic values of groundwater levels at W0 under different future simulation scenarios (2025–2040). Text S1. Detailed field methodologies for groundwater monitoring well installation and sampling. Figure S1 Hydrogeological cross-section. Table S3: Specifications of the constructed groundwater monitoring wells.

Author Contributions: Conceptualization, T.L. and T.W.; software, N.W. and Y.H.; validation, H.G., N.W. and Y.H.; resources, S.Z., T.L., X.M. and D.Z.; writing—original draft preparation, T.L. and S.Z.; supervision, T.W.; funding acquisition, T.W. All authors have read and agreed to the published version of the manuscript.

Funding: This research was funded by the Natural Science Foundation of Henan (No. 252300421460) and the Investigation and Assessment of Groundwater Environmental Conditions in Landfill Sites of Henan Province and Integration of "Two Sites" Achievements Project (No.20241058A).

Data Availability Statement: The model-driven data (precipitation and evaporation) were obtained from the ERA5 reanalysis product (https://www.ecmwf.int/en/forecasts/dataset/ecmwf-reanalysis-v5, accessed on 1 May 2025), while the remaining observed data are presented in the text.

Acknowledgments: We sincerely thank Shujie Hu and Zhuoqian Li from the Ecological Environment Geo-Service Center of Henan Geological Bureau for their invaluable guidance and constructive suggestions throughout the preparation of this manuscript. We are grateful to the three anonymous reviewers and the guest editor for the Special Issue, Siarkos, for their numerous constructive comments on this study, which helped significantly improve the quality of this paper.

Conflicts of Interest: Authors Tengchao Li, Shengyan Zhang, Xiaoming Mao and Daoyuan Zheng were employed by the Ecological Environment Geo-Service Center of Henan Geological Bureau. The remaining authors declare that the research was conducted in the absence of any commercial or financial relationships that could be construed as potential conflicts of interest.

References

1. Liu, J. Prediction and Optimization of Municipal Solid Waste Production and Heating Values Based on Machine Learning. Master's Thesis, Beijing Foreign Studies University, Beijing, China, 2023.
2. Fang, K.; Xiong, Z.; Lu, M.; Li, T.; Li, J. Advances in New and Renewable Enengy. *Adv. New Renew. Enengy* **2019**, *7*, 359–364.
3. Wang, J.; Dan, Z.; Zhou, W.; Zhu, K.; Shang, X.; Wan, X.; Zheng, Z. Analysis of the changing trend of main ways of domestic waste disposal in different regions of China. *Recycl. Res.* **2024**, *17*, 12–17.
4. Zhang, J.; Zheng, M.; Zheng, F.; Yang, J.; Zheng, Y. Characterization of domestic waste leachate generation, treatment methods, and development trends in China: A comprehensive review. *Chin. J. Environ. Eng.* **2025**, 1–19.
5. Renou, S.; Givaudan, J.G.; Poulain, S.; Dirassouyan, F.; Moulin, P. Landfill leachate treatment: Review and opportunity. *J. Hazard. Mater.* **2008**, *150*, 468–493. [CrossRef] [PubMed]
6. Liu, Y. Emissions of Non-Methane Organic Compounds from Municipal Solid Waste Landfills and Their Air Dispersion Modeling. Ph.D. Thesis, Tsinghua University, Beijing, China, 2017.
7. Zhao, L. Migration Rules and Control Methods of Groundwater Contaminants at Valley-Type Landfill Sites. Ph.D. Thesis, Zhejiang University, Hangzhou, China, 2024.
8. Li, H. Degradation-Consolidation Behaviors and Treatment Methods for the Liquid-Gasinduced Environmental Disaster of High-Food-Waste-Content MSW Landfill. Ph.D. Thesis, Zhejiang University, Hangzhou, China, 2021.
9. Ye, J.; Chen, X.; Chen, C.; Bate, B. Emerging sustainable technologies for remediation of soils and groundwater in a municipal solid waste landfill site—A review. *Chemosphere* **2019**, *227*, 681–702. [CrossRef]
10. Kamaruddin, M.A.; Yusoff, M.S.; Rui, L.M.; Isa, A.M.; Zawawi, M.H.; Alrozi, R. An overview of municipal solid waste management and landfill leachate treatment: Malaysia and Asian perspectives. *Environ. Sci. Pollut. Res.* **2017**, *24*, 26988–27020. [CrossRef]
11. Liu, D.; Yu, X.; Luo, Y.; Sun, J.; Jiang, D.; Tan, Z. Analysis of Leachate Characteristics from Municipal Solid Waste Landfills. *Environ. Sci. Technol.* **2006**, *6*, 55–57+118. [CrossRef]
12. Siddiqua, A.; Hahladakis, J.N.; Al-Attiya, W.A.K.A. An overview of the environmental pollution and health effects associated with waste landfilling and open dumping. *Environ. Sci. Pollut. Res.* **2022**, *29*, 58514–58536. [CrossRef]
13. Chen, C. A Method for Evaluating Performances of Composite Liners Considering Random Distributions of Holes and Wrinkles. Ph.D. Thesis, Zhejiang University, Hangzhou, China, 2018.
14. Yang, W. ComGIS-Based Simulation and Prediction of Groundwater Pollution in Landfill Site. Master's Thesis, Hefei University of Technology, Hefei, China, 2018.
15. Wang, Y. Hilly Area of a Domestic Waste Landfill Area Water Health Risk Prevention and Control Countermeasures. Master's Thesis, Jilin University, Changchun, China, 2024.
16. Yu, X.; Sui, Q.; Lyu, S.; Zhao, W.; Cao, X.; Wang, J.; Yu, G. Do high levels of PPCPs in landfill leachates influence the water environment in the vicinity of landfills? A case study of the largest landfill in China. *Environ. Int.* **2020**, *135*, 105404. [CrossRef] [PubMed]
17. Wu, L.; Zhan, L.; Lan, J.; Chen, Y.; Zhang, S.; Li, J.; Liao, G. Leachate migration investigation at an unlined landfill located in granite region using borehole groundwater TDS profiles. *Eng. Geol.* **2021**, *292*, 106259. [CrossRef]
18. Han, Z.; Ma, H.; Shi, G.; He, L.; Wei, L.; Shi, Q. A review of groundwater contamination near municipal solid waste landfill sites in China. *Sci. Total Environ.* **2016**, *569–570*, 1255–1264. [CrossRef]
19. Zhan, L.; Wu, L.; Han, H.; Zhang, S.; Zhou, H.; Song, X.; Zhao, L.; Guo, Q.; Chen, Y. Hydrogeological classification of municipal solid waste landfill sites in China and correlation with groundwater contaminant migration. *Hydrogeol. J.* **2023**, *31*, 771–787. [CrossRef]
20. Zhan, L.; Zhao, R.; Wu, L.; Zhang, Y. Estimation of migration distance of groundwater pollutants at plain-type unlined MSW landfill sites. *J. Saf. Environ.* **2025**, *25*, 1958–1968. [CrossRef]
21. Peng, Q.; Huang, P.; Chen, D.; Zhu, D. Distribution and change of China's population on the terrain gradientsfrom 2000 to 2020. *Prog. Geogr.* **2023**, *42*, 2019–2032. [CrossRef]
22. Jia, C.; Yang, X.; Liu, S.; Wang, S.; Wang, H.; Liu, J. Environmental Impact of Landfill on Groundwater Quality Based on Indexanalysis and Gis Method. *Environ. Eng.* **2021**, *39*, 156–163+155. [CrossRef]
23. Zhao, Y.; Zhang, M.; Liu, Z.; Ma, J.; Yang, F.; Guo, H.; Fu, Q. How Human Activities Affect Groundwater Storage. *Research* **2024**, *7*, 0369. [CrossRef]
24. Dao, P.U.; Heuzard, A.G.; Le, T.X.H.; Zhao, J.; Yin, R.; Shang, C.; Fan, C. The impacts of climate change on groundwater quality: A review. *Sci. Total Environ.* **2024**, *912*, 169241. [CrossRef] [PubMed]
25. Xie, H.; Chen, Y.; Zhu, X.; Bouazza, A.; Yan, H. Numerical simulation of different pollutant control measures around an old landfill contaminated site: A field scale study. *J. Environ. Manag.* **2023**, *348*, 119350. [CrossRef]
26. Shinwari, F.U.; Liaquat, U.; Khan, M.A.; Kontakiotis, G.; Makri, P.; Lianou, V.; Antonarakou, A. Hydrochemical zonation and depth-based vulnerability of groundwater in Islamabad using GIS and WQI techniques. *Front. Water* **2025**, *7*, 1581668. [CrossRef]

27. Han, J. Groundwater Environment Impact Assessment and Prediction of a Garbage Dumpling Based on GMS. Master's Thesis, Hefei University of Technology, Hefei, China, 2016.
28. Sykes, J.F.; Pahwa, S.B.; Lantz, R.B.; Ward, D.S. Numerical simulation of flow and contaminant migration at an extensively monitored landfill. *Water Resour. Res.* **1982**, *18*, 1687–1704. [CrossRef]
29. Meng, M.; Wen, Z.; Luo, W.; Wang, S. Approaches and Policies to Promote Zero-Waste City Construction: China's Practices and Lessons. *Sustainability* **2021**, *13*, 13537. [CrossRef]
30. Niu, J.; Hu, L.; Zhang, M. Transport of ammonia nitrogen for groundwater pollution control in an informal low-permeability landfill site. *Hydrol. Res.* **2022**, *53*, 370–384. [CrossRef]
31. Zheng, C. MT3D: A modular three-dimensional transport model for simulation of advection, dispersion and chemical reactions of contaminants in groundwater systems. In *Report to the Kerr Environmental Research Laboratory*; US Environmental Protection Agency: Ada, OK, USA, 1990.
32. Zheng, C. Recent Developments and Future Directions for MT3DMS and Related Transport Codes. *Groundwater* **2009**, *47*, 620–625. [CrossRef]
33. Meng, J.; Xiao, G.; Qi, M.; Han, X.; Gou, Q.; Hao, X.; Ge, J. Comparing roles of multiple contamination indicators in tracing groundwater pollution nearby a typical municipal solid waste (MSW) landfill. *Heliyon* **2024**, *10*, e35601. [CrossRef] [PubMed]
34. Cao, G.; Zheng, C.; Scanlon, B.R.; Liu, J.; Li, W. Use of flow modeling to assess sustainability of groundwater resources in the North China Plain. *Water Resour. Res.* **2013**, *49*, 159–175. [CrossRef]
35. Muñoz-Sabater, J.; Dutra, E.; Agustí-Panareda, A.; Albergel, C.; Arduini, G.; Balsamo, G.; Boussetta, S.; Choulga, M.; Harrigan, S.; Hersbach, H.; et al. ERA5-Land: A state-of-the-art global reanalysis dataset for land applications. *Earth Syst. Sci. Data* **2021**, *13*, 4349–4383. [CrossRef]
36. Tarek, M.; Brissette, F.P.; Arsenault, R. Evaluation of the ERA5 reanalysis as a potential reference dataset for hydrological modelling over North America. *Hydrol. Earth Syst. Sci.* **2020**, *24*, 2527–2544. [CrossRef]
37. Iribar, V.; Carrera, J.; Custodio, E.; Medina, A. Inverse modelling of seawater intrusion in the Llobregat delta deep aquifer. *J. Hydrol.* **1997**, *198*, 226–244. [CrossRef]
38. Pool, M.; Post, V.E.A.; Simmons, C.T. Effects of tidal fluctuations and spatial heterogeneity on mixing and spreading in spatially heterogeneous coastal aquifers. *Water Resour. Res.* **2015**, *51*, 1570–1585. [CrossRef]
39. Siarkos, I.; Mallios, Z.; Tzoraki, O.; Latinopoulos, P. A methodological framework for the optimal design of injection barriers against seawater intrusion in coastal-rural regions. *Sci. Total Environ.* **2025**, *966*, 178679. [CrossRef]
40. *GB/T 14848-2017*; Groundwater Quality Standard of the People's Republic of China. AQSIQ: Beijing, China, 2017.
41. Sinnathamby, G.; Phillips, D.H.; Paksy, A.; Halim, M. Landfill cap models under simulated climate change precipitation: Assessing long-term infiltration using the HELP model. *Environ. Earth Sci.* **2024**, *83*, 311. [CrossRef]
42. Masoner, J.R.; Cozzarelli, I.M. Spatial and Temporal Migration of a Landfill Leachate Plume in Alluvium. *Water Air Soil Pollut.* **2015**, *226*, 18. [CrossRef]
43. Di Palma, L.; Mecozzi, R. Batch and column tests of metal mobilization in soil impacted by landfill leachate. *Waste Manag.* **2010**, *30*, 1594–1599. [CrossRef]
44. Wang, J.; Qiao, Z. A comprehensive review of landfill leachate treatment technologies. *Front. Environ. Sci.* **2024**, *12*, 1439128. [CrossRef]
45. Linh, H.N.; Tamura, H.; Komiya, T.; Saffarzadeh, A.; Shimaoka, T. Simulating the impact of heavy rain on leaching behavior of municipal solid waste incineration bottom ash (MSWI BA) in semi-aerobic landfill. *Waste Manag.* **2020**, *113*, 280–293. [CrossRef]
46. Huang, Z.; Liu, G.; Zhang, Y.; Yuan, Y.; Xi, B.; Tan, W. Assessing the impacts and contamination potentials of landfill leachate on adjacent groundwater systems. *Sci. Total Environ.* **2024**, *930*, 172664. [CrossRef] [PubMed]
47. Ahmadi, H.; Kilanehei, F.; Nazari-Sharabian, M. Impact of Pumping Rate on Contaminant Transport in Groundwater—A Numerical Study. *Hydrology* **2021**, *8*, 103. [CrossRef]
48. Wang, T.; Wu, Z.; Wang, P.; Wu, T.; Zhang, Y.; Yin, J.; Yu, J.; Wang, H.; Guan, X.; Xu, H.; et al. Plant-groundwater interactions in drylands: A review of current research and future perspectives. *Agric. For. Meteorol.* **2023**, *341*, 109636. [CrossRef]
49. Şengör, S.S.; Ünlü, K. Colloidal transport of heavy metals in low-advective-velocity environmental systems: Reactive transport model on biogeochemical and hydrodynamic impacts. *Vadose Zone J.* **2023**, *22*, e20233. [CrossRef]

Disclaimer/Publisher's Note: The statements, opinions and data contained in all publications are solely those of the individual author(s) and contributor(s) and not of MDPI and/or the editor(s). MDPI and/or the editor(s) disclaim responsibility for any injury to people or property resulting from any ideas, methods, instructions or products referred to in the content.